01,07

Thermodynamic parameters of crystallization during heating of metallic amorphous metal-metalloid alloys

© L.V. Spivak, N.E. Shchepina, I.V. Lunegov

Perm State University,
Perm, Russia

E-mail: lspivak2@mail.ru

Received March 23, 2025
Revised March 28, 2025
Accepted March 29, 2025

For the first time, high-resolution differential scanning calorimetry provides information on the enthalpy and entropy of crystallization stages during heating of amorphous metal alloys (AMA) metal-metalloid based on iron and cobalt $Fe_{77}Ni_1Si_9B_{13}$ and $Fe_5Co_{58}Ni_{10}Si_{11}B_{16}$. The thermodynamic characteristics of AMA during crystallization and of the basic elements Fe and Co during their crystallization from the melt have been analyzed. In all cases without exception, the enthalpy and entropy values of AMA crystallization are markedly smaller than those of base elements crystallization from the melt. The activation energies of phase transformation during heating of AMA at the first and second stages of their realization have been determined. A marked effect of heating rate (5−40 K/min) on the enthalpy and entropy of crystallization of the Co-based metal-metalloid alloy was found. It is shown that maturation of an iron-based alloy at room temperature for 10 years leads to a noticeable decrease in the exothermic effect of its crystallization while preserving the two-stage character of such transformation.

Keywords: calorimetry, enthalpy, entropy, activation energy, amorphous state.

DOI: 10.61011/PSS.2025.04.61260.60-25

1. Introduction

A considerable number of publications and separate monographs have been devoted to the study of crystallization processes (phenomena) during heating of amorphous metal alloys (AMA). Some results of numerous studies are integrated, for example, in Refs. [1,2]. However, comparison of the crystallization patterns of AMA with those of metallic melts has been found to have received much less attention. *A priori* is clear that crystallization from a melt occurs at a substantially lower thermodynamic stimulus than for such a transformation in AMA. Second, in the case of crystallization of melts, which most often occurs during their cooling from certain temperatures, both the thermodynamic stimulus of the phase transition and the diffusional mobility of atoms involved in the rearrangement of the structure are differently directed. In the case of AMA crystallization, they are equidirectional and increase with the increase of the temperature of the amorphous matrix. Thirdly, the crystallization centers that have arisen during the cooling of melts grow in a medium (liquid phase) with relatively weak resistance to the growth of particles of the new phase, whereas during the crystallization of AMA, the growth of crystallization centers occurs in a medium whose viscosity is orders of magnitude higher than in the liquid phase. And, lastly, as shown in Ref. [1], the diffusive mobility of metallic atoms is higher and metalloidal atoms lower in AMA than in their crystalline counterparts.

The use of differential scanning calorimetry (DSC) techniques in the study of crystallization from melts is often used to determine important thermodynamic parameters such as enthalpy and entropy of the phase transition. However, we did not find in the literature any data on the determination of the enthalpy and entropy of phase transformations responsible for the transition of the amorphous matrix to the crystalline state, particularly in alloys $Fe_{77}Ni_1Si_9B_{13}$ and $Fe_5Co_{58}Ni_{10}Si_{11}B_{16}$. In rare cases, the temperature intervals of crystallization steps and, even more rarely, the activation energy of such transformations have been determined on the basis of DSC studies [3–9]. A comparison of these two types of crystallization, in AMA crystallization and melt crystallization, formed one aspect of the present study.

2. Research methodology

Metal-metalloid alloys of the following composition were studied: $Fe_{77}Ni_1Si_9B_{13}$ (designation in mass production — 2HCP), molar weight 47.98 g/mol, and $Fe_5Co_{70}Si_{15}B_{10}$ (designation in mass production — 71K), molar weight 49.3 g/mol. The alloys were obtained by planar casting. The cooling rate is $\sim 10^6$ K/min. Tape thickness is 40×50 mcm.

The surface was studied on the free (non-contact) surface of the tape. A Ntegra Prima atomic force microscope with a high-resolution scanning head 1×1 mcm and a NSG-01Au gold-coated cantilever with a tip diameter not exceeding 1 nm was used. A semi-contact topography method is implemented in scanning. The cantilever was tuned to an operating resonant frequency of 150 kHz with a signal amplitude of 25 nÅ. The scanning speed was chosen with consideration of the surface topography and

cantilever sensitivity. The resulting scans were processed programmatically to remove noise and surface slope.

The differential scanning calorimetry measurements were performed using analyzer Netzsch STA „Jupiter“ 449. Heating and cooling were performed in argon environment 5, 10, 20 and 40 K/min in the argon environment (99.998% Ar). Gas flow rate 25−30 ml/min. The masses of the samples were within the range of 15−20 mg.

Proteus Analyses software and the Fityk package were used for processing of experimental DSC data, including the determination of critical point temperatures. We reduced the impact of factors difficult to account for on DSC measurements by approximating the experimental DSC signal dependence by a 6-8th degree DSC polynomial.

3. Experimental findings and their discussion

Figure 1 shows the DSC data for the 2NSR alloy obtained at different heating rates. The so-called reduced heat capacity C_{Pexcess} is plotted on the ordinate axis, which comprises the DSC analysis data normalized to the heating rate (β) and mass (m_s) of the samples (see [10]):

$$C_{\text{P}_{\text{excess}}} = \frac{\dot{Q}_s - \dot{Q}_{\text{Bl}}}{m_s \beta}, \quad \text{Jg}^{-1}\text{K}^{-1}. \tag{1}$$

Here $\dot{Q}_s$ and $\dot{Q}_{\text{Bl}}$ are heat fluxes during heating with sample and base heat fluxes, respectively.

A typical form of this dependence is observed for metal-metalloid alloys containing less than 17 at.% metalloid [1]: bifurcation of the exothermic crystallization effect into two sections with different rates of heat release. With the increase of the heating rate, a shift of the corresponding maxima P_1 and P_2 toward higher temperatures is observed. The latter allows us (see [11]) to estimate the activation energy of the processes responsible for the occurrence of such maxima on the DSC curves.

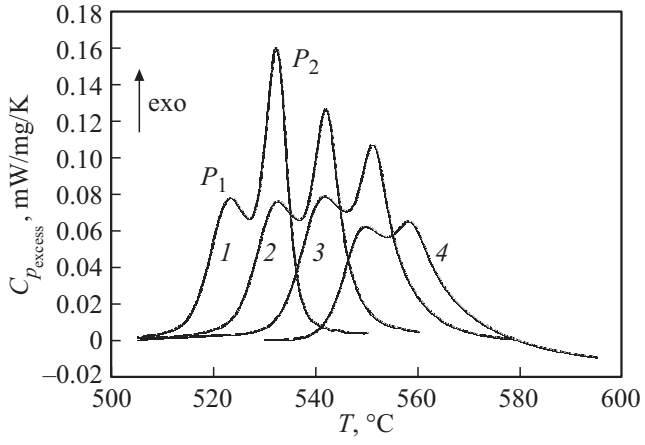

Figure 1. Effect of heating rate on DSC signal variation during heating of AMA 2NSR. Heating rate: curve *1* — 5, *2* — 10, *3* — 20, *4* — 40 K/min.

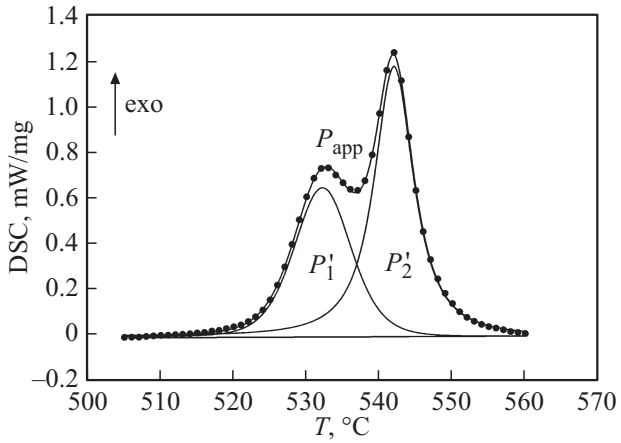

Figure 2. The structure of the exothermic effect during heating at a rate of 10 K/min AMA 2NSR. Experimental data are shown by dots; P_{app} — approximation result; P_1' and P_2' are subpeaks.

These values were found to be close for both crystallization processes: low-temperature $E_1 = 430 \pm 20$ kJ/mol, high-temperature $E_2 = 420 \pm 20$ kJ/mol. 208 kJ/mol was obtained for the first process in the alloy $Fe_{34}Co_{26}Si_6B_{14}$ for the transformation of α-(Fe,Co) in Ref. [3], which is significantly less than for the cobalt-free alloy (transformation α-(Fe,Si)). An activation energy value of 390 kJ/mol was obtained (see Ref. [4]) for the first crystallization step in $Fe_{77.5}Si_{13.5}B_9$ alloy, and the activation energy was 400 kJ/mol for the second step. These values are quite close to those we obtained on an alloy with nearly the same iron content.

We decomposed the exothermic effect on the DSC curves into the corresponding subpeaks P_1' and P_2' for estimating the partial contribution to the total balance of the exothermic crystallization effect of each of the phase transformation mechanisms. An example of this decomposition is shown in Figure 2. This procedure was implemented for each heating rate: 5−10−20−40 K/min.

Naturally, the temperatures of all extreme points P_1' and P_2' shift to the higher temperature region as the heating rate increases. Heating rate affects process enthalpy ΔH and configurational entropy ΔS. The enthalpy of the transformation for the P_1' process decreases from 2.1 to 1.0 kJ/mol as the heating rate increases and the entropy of such a transition decreases correspondingly, from 2.4 to 1.2 J/(mol · K). The enthalpy and entropy of such a transition increase for the P_2' process with the increase of the heating rate, respectively, from 2.5 to 3.4 kJ/mol and from 3.2 to 4.1 J/(mol · K). The transformation P_1' decreases its contribution to the total exothermic effect of the transformation with the increase of the heating rate, and the transformation P_2' increases it.

Based on the entropy values, the state of the AMA before the transformation P_1' can be considered more ordered than the state of the system before the P_2' process. This is probably a consequence of the fact that „frozen“ crystallization centers exist in the matrix in the amorphous state, the presence of which has been postulated in numerous studies

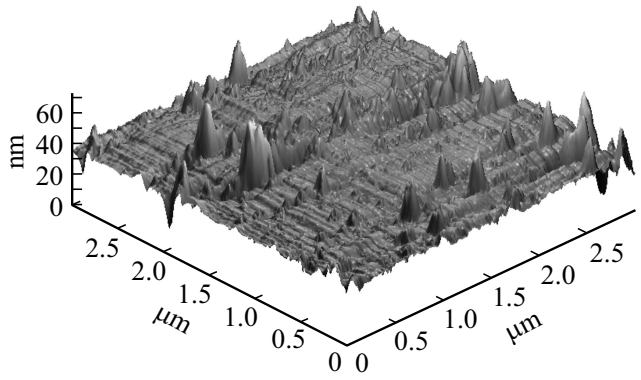

Figure 3. Surface structure of 2NSR alloy in the amorphous state.

(see, for example, [12–21]). Ref. [12] should be considered as one of the first studies that made this assumption.

A comparison of enthalpy and entropy during crystallization of this AMA with its value during crystallization of iron from the melt as the basic element of this alloy has been made. For pure iron, $\Delta H = 13.8\,\text{kJ/mol}$ and $\Delta S = 7.6\,\text{J/(mol}\cdot\text{K)}$ [22]. Since the iron in this AMA is 78 at.%, it can be assumed that the enthalpy and entropy of transformation under these conditions should be about $10-11\,\text{kJ/mol}$ and $6\,\text{J/(mol}\cdot\text{K)}$, respectively, in case of crystallization from the liquid state of this alloy.

If one considers that the configurational entropy is a measure of shuffling of atoms during the transition of the system from one state to another, then the transition from a disordered state with near-order to far-order in the case of ordinary crystallization is associated with a more pronounced shuffling of atoms than in the case of crystallization of amorphous alloys. At least two explanations can be proposed for this. The first is attributable to the large thermodynamic stimulus of phase transformation, and the second is attributable to the fact that in AMA, ribbons of formation are observed on the surface immediately after fabrication, which can be regarded as „frozen" crystallization centers. They seem to be registered in our studies as well (Figure 3).

The size of such formations does not exceed 20 nm in height and 100 nm in diameter. It is clear that such formations are not detected at the resolving power of conventional differential X-ray spectroscopy. Therefore, such an alloy is considered „X-ray amorphous". These formations („frozen" crystallization centers) usually are not present in case of crystallization of metallic melts.

The presence of such features of structure in rapidly quenched metal-metalloid alloys already initially raised the question of the stability of their state. A separate chapter was devoted to this question already in Ref. [1]. However, as was apparent from Ref. [1] and the numerous studies that followed in this direction (see, for example, [23]), it all came down to the influence of various factors on the devitrification temperature T_x. If we refer to one of the recent studies of AMA stability (see [5]), it refers to the study of this phenomenon in massive metal-to-metal AMA systems. As a conclusion, it shows that most of the studied metallic glasses stored under ambient conditions for more than 15 years retained the original silvery metallic color and the original either vitreous or partially crystalline structure. No visible changes were found in the X-ray images. Transmission electron microscopy observations also confirmed the preservation of vitreous structure in the alloys. Although the crystallization temperature slightly decreased after more than 15 years of natural ageing, but the decrease was only a few kelvins.

We also had the largely unique opportunity to compare the behavior of the same alloy 10 years after its fabrication. Figure 4 shows the DSC dependencies of this alloy immediately after fabrication and after 10 years of ageing at room temperature. The results obtained speak for themselves. Such an alloy relaxes to some state of thermodynamic equilibrium during the entire observation process. Control measurements were made after 3 years and after 6 years of ageing.

It can be seen from the data shown in Figure 4 that two stages of crystallization are preserved and the thermal effect of crystallization significantly decreased after 10 years of ageing at room temperature. In addition, the P_1 process has a greater contribution to the total heat flux than was recorded at the initial time of observation. The temperature of the maximum rate of the occurrence of the first stage of crystallization slightly decreases (3 °C), while the temperature of the maximum rate of occurrence of the second stage slightly increases (11 °C).

And in this case, the thermal effect of crystallization can be represented as a superposition of two effects realized in close and overlapping temperature ranges.

The specific calculation results for this case are as follows.

- Initial state:

  P'_1 $\Delta H = 2.0\,\text{kJ/mol}$, $\Delta S = 2.3\,\text{J/(mol}\cdot\text{K)}$;

  P'_2 $\Delta H = 2.6\,\text{kJ/mol}$, $\Delta S = 3.5\,\text{J/(mol}\cdot\text{K)}$.

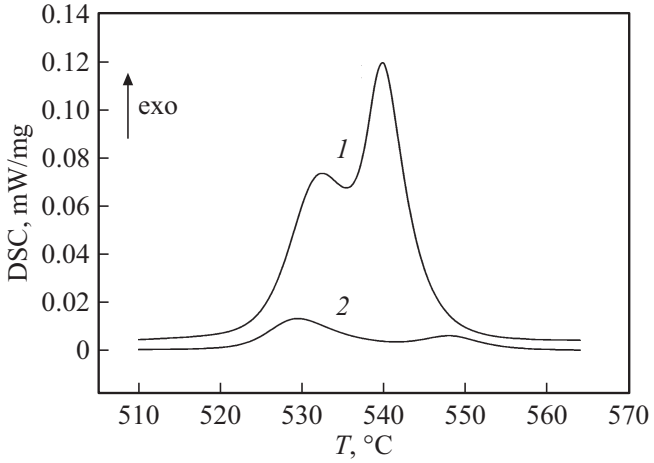

Figure 4. The effect of ageing at room temperature on the appearance of the DSC signal in case of heating of AMA 2NSR. Heating rate of 10 K/min. Initial condition is shown by curve *1, 2* shows the condition after 10 years of storage.

- After ageing:
  P_1' $\Delta H = 0.4\,\text{kJ/mol}$, $\Delta S = 0.5\,\text{J/(mol}\cdot\text{K)}$;
  P_2' $\Delta H = 0.2\,\text{kJ/mol}$, $\Delta S = 0.2\,\text{J/(mol}\cdot\text{K)}$.

The obtained values of ΔH and ΔS show that there is a difference in the structural structure of the amorphous alloy before crystallization at the initial time and after its ageing.

It was important to identify the type of phase transitions responsible for the occurrence of exothermic maxima, P_1 and P_2. One such method [24–26] is to compare the temperatures of the maxima of the DSC signal and the maximum of its second derivative in temperature. The following was found. This discrepancy was $1.1 \pm 0.2\,^\circ\text{C}$ for peak P_1 on average at all heating rates; the divergence was $0.6 \pm 0.2\,^\circ\text{C}$ for peak P_2; the divergence was $0.4 \pm 0.1\,^\circ\text{C}$ for peak P_1'; the divergence was $0.3 \pm 0.1\,^\circ\text{C}$ for peak P_2'. From this we can see that the maximum divergence is about $1\,^\circ\text{C}$ for the original DSC signal and only $0.5\,^\circ\text{C}$ for the peaks obtained by decomposing the DSC signal into two subpeaks. The latter should be considered an operation that more adequately reflects the real situation. The given data allow us to assert that the appearance of the peaks P_1 and P_2 is a consequence of the processes occurring during the realization of phase transitions of kind I. This difference between the temperatures of the extreme points tends to increase to some extent with the increase of the heating rate, but remains within the limits of consistency with the conclusions drawn.

There is another approach to the consideration of phase transformation mechanisms, which is that the DSC curves in the heating regime are characterized by the reaction order parameter at a given phase transition (see [11]).

The reaction order n can be determined from the relation given in Ref. [11]:

$$n = 1.26\sqrt{S}. \tag{2}$$

Here S is the shape factor of the DSC curve in the region of the thermal effect registration temperatures: the ratio of the tangent slope tangents at the inflection points of the experimental DSC dependence.

Shapes of DTA [27] and DSC [28,29] curves were theoretically calculated for different mechanisms of phase transformation: diffusion, reaction at the phase interface, nuclei growth process. Of these, the reaction order is $n < 1$ for the first two mechanisms, taking into account the form factor. $n \to 1.3$ for the process controlled by nucleus growth. In this case, the dependence $\frac{d\alpha}{dT}(T)$, where $\frac{d\alpha}{dt}$ is reaction rate, passes through a maximum and is ideally a symmetric curve ($S = 1$). The mean value of the order parameter n for the process P_1' is found to be 1.3 ± 0.1. The mean of n for the process P_2' turned out to be 1.4 ± 0.1. Consequently, the transformations P_1' and P_2' belong to the phase transformation of kind I and develop by nucleation and growth of new phase embryos.

These values of the order parameter n were found to be 1.5 and 1.2, respectively, after 10 years of ageing. That is, ageing has virtually no effect on the characteristics of such a transition. It can be noted that for the first variant of the evaluation of the type of phase transition in the alloy after 10 years of ageing the discrepancy between the extreme points for the process P_1 was $0.2\,^\circ\text{C}$, for the process P_2 was $0.3\,^\circ\text{C}$.

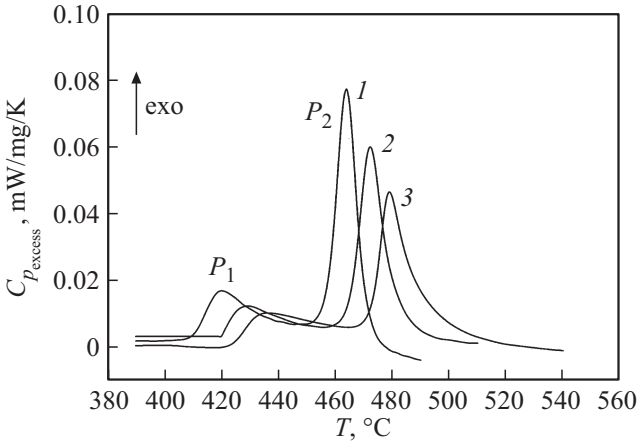

Figure 5. The effect of heating rate on the change of DSC signal in case of heating of AMA $Fe_5Co_{58}Ni_{10}Si_{11}B_{16}$. Curve *1* — 10, *2* — 20, *3* — 40 K/min.

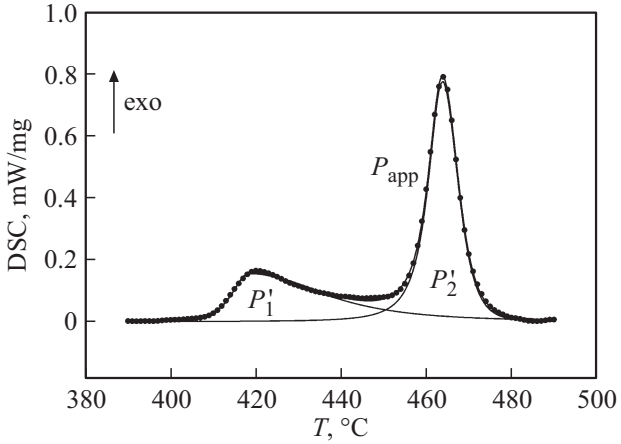

Figure 6. The structure of the exothermic effect in case of heating of AMA $Fe_5Co_{58}Ni_{10}Si_{11}B_{16}$ at rates of 10 K/min. The experimental data are shown by dots; P_{app} is the approximation result; P_1' and P_2' — subpeaks.

Figure 5 shows the effect of heating rate on the appearance of the DSC dependence for cobalt-based AMA (71K). A splitting of the exothermic crystallization effect of this alloy upon heating is observed like in case of AMA 2NSR. These two maxima of the heat release rate shift to the higher temperature region with the increase of the heating rate. Evaluation of the activation energies of the processes responsible for the appearance of the maxima P_1 and P_2 shows that these values were found to be $E_1 = 340 \pm 25\,\text{kJ/mol}$, $E_2 = 410 \pm 20\,\text{kJ/mol}$. The partial contribution of each process (Figure 6) to the total thermal effect of the transformation is characterized by the following features for heating at different rates.

The enthalpy value ΔH changes from 480 to 2450 kJ/mol for the process P_1' with the increase of the heating rate, entropy ΔS changes from 0.7 to $6.5\,\text{J/(mol}\cdot\text{K)}$. Accordingly,

for the process P_2' ΔH changes from 536 to 4800 kJ/mol, the entropy ΔS changes from 0.3 to 2.0 J/(mol · K). These characteristics markedly differ from those obtained for the 2NSR alloy depending on the heating rate. This appears to be attributable to the presence of cobalt as a major component of this amorphous alloy.

The temperature difference between the maximum of the temperature derivative of the second derivative of the DSC signal and the maximum of the DSC signal (and the maximum of the DSC signal after splitting the thermal effect into its components) for all heating rates is as follows: for peak P_1' $0.3 \pm 0.1\,^{\circ}$C, for peak P_2' $0.4 \pm 0.1\,^{\circ}$C. Thus, the processes causing the occurrence of peaks P_1' and P_2' can be attributed, formally, to phase transformations of kind I.

The parameter value of the order of $n = 2.8 \pm 0.2$ was obtained for the amorphous alloy $Fe_5Co_{58}Ni_{10}Si_{11}B_{16}$ for the process P_1' (asymmetric peak DSC), which is not found in the literature. The mean value is $n = 1.4 \pm 0.2$ for the process P_2'. There is some trend of decreasing n for process P_1', and its increasing for process P_2' with increasing heating rate.

The following processes occur during heating of quenched amorphous alloys of the metal-metalloid system according to the existing concepts: first, a highly dispersed metastable phase MS-I is released in the amorphous phase, then this mixed structure completely transforms into a crystalline metastable phase MS-II, which transforms at higher temperatures into a stable equilibrium structure ST. The MS-I phase comprises small crystals of solid solution on the base metal. The MS-II phase grows very rapidly from this conglomerate of crystalline and amorphous constituents, due to irregular nucleation, resulting in the complete disappearance of the amorphous matrix. The structure of this phase in the case of low temperature of formation is homogeneous, and in the case of high temperature is a eutectoid type structure. The low-temperature maximum on DSC corresponds to the formation of the MS-I phase, and the high-temperature maximum corresponds to the MS-II phase. The following transformations take place schematically: Am → MS-I → MS-II → ST. The MS-II phase is probably close to chemical compounds of the type M_3X (M is metal, X is metalloid).

As shown in Figure 5, a clear asymmetry of the peak P_1 is observed in case of the crystallization of the 71 K alloy. Most likely, the shape of the exothermic signal (high value of the order parameter n) is in this case a consequence of the development of the transformation according to the Lifshitz-Slezov theory [30]: in the diffusion process of forming a new phase during the decomposition of a supersaturated solid solution, it should be borne in mind that there is a coalescence stage along with the stages of particle nucleation and growth. The first two stages involve the fluctuating formation of new phase nuclei and their further growth directly from the solid solution.

The coalescence process prevails at the stage of growth of new phase particles, when their size is already large enough, and at the same time the supersaturation of the solid solution of the matrix phase becomes small and the fluctuation nucleation of a new phase is practically excluded (the critical size of nucleates should reach a macroscopic value). The mechanism of the coalescence process comprises the growth of large particles due to the dissolution of small particles, resulting in the total particle volume of the new phase remaining unchanged on the asymptotics of the process. It should be noted that the role of coalescence processes in AMA crystallization was first pointed out by Stoltenberg [31].

The theoretical analysis of the one- and two-step crystallization process carried out in Ref. [32] also showed that the occurrence of other kinetic processes with thermal effects in AMA can lead to the asymmetry of the corresponding peaks on DSC thermograms during the transition from the amorphous state to the crystalline state.

4. Conclusion

The use of DSC-analysis to obtain information on the enthalpy and entropy of phase transformation at the first and second stages of the transition of amorphous matrix into crystalline matrix, in contrast to structural methods, makes it possible to identify the effects characterizing the ongoing changes in the entire volume of the undergoing transformation of the material. It follows from the above DSC data for AMA 2NSR and 71K that the transition in the first stage of crystallization of these metal-to-metalloid alloys is characterized by less atom shuffling than is typical of the second stage of crystallization. This appears to be attributable to the fact that solid solution crystals are produced from the amorphous matrix in the first stage, whereas a chemical compound with a more complex spatial organization of the atomic structure is produced in the second stage. The relatively low values of configurational entropy in the first stage of crystallization may also be a consequence of the greater degree of structural organization in the amorphous state as opposed to dense random packing models [33], even more so in the liquid phase.

It should be noted that a more pronounced dependence of thermodynamic parameters on heating rate is observed in Co-based AMA than in Fe-based AMA. Apparently, this is attributable to the specific role of Co, the presence of which in AMA is considered as a stabilization factor of the amorphous state [33,34].

From practical point of view, it is shown that, on the basis of data on the ageing of 2NSR alloy at ordinary temperatures, it should be assumed that alloys of this system relax for long periods of time to a thermodynamically stable state immediately after fabrication. At the same time, no significant changes occur in metal-to-metal AMA even when they are aged for 15 years. A different diffusional mobility of metalloid and metal atoms in AMC can be a possible reason for this discrepancy [1].

Both the first and the second stages of crystallization of the studied 2NSR and 71K alloys belong to phase transitions of kind I and develop through the formation

of crystallization centers and their further growth. This transition is characterized by the spontaneous formation of smaller crystallization centers and, to a much lesser extent, the development of the transformation by their growth. Some parallel with the discovered features of crystallization of two-component alloys can be seen in this [35]. Another stage is also possible in alloy 71K that is associated with the coalescence of the structure elements formed during the realization of the first stage.

5. Conclusions

The information about the enthalpy and entropy values for the two-step crystallization of iron- and cobalt-based metal-to-metalloid AMA have been obtained. The possibility to describe on the basis of this information the features of transformation of the AMA structure during the transition from the amorphous state to the crystalline state is shown: the shuffling of atoms is less pronounced during the crystallization of AMA in comparison with the crystallization of metallic melts.

The activation energies of phase transformations at the first and second stages of crystallization of these AMA during heating have been determined. Their magnitudes indicate the diffusive nature of the mechanisms controlling the shuffling of atoms in such transformations.

Prolonged ageing at room conditions does not affect the two-step character of crystallization processes in case of heating of AMA 2NSR, but significantly reduces the thermal effect of the transformation.

Conflict of interest

The authors declare no conflict of interest.

References

[1] K. Suzuki, H. Fujimori, K. Hashimoto. Materials Science of Amorphous Metals / Ed. T. Masumoto. Ohmsha, Tokyo (1982). 281 p.

[2] D.V. Louzguine-Luzgin. Mater. **17**, *14*, 3573 (2024). https://doi.org/10.3390/ma17143573

[3] I.C. Rho, C.S. Yoon, C.K. Kim, T.Y. Byun, K.S. Hong. J. Non-Cryst. Solids **316**, *2–3*, 289 (2003).

[4] S.D. Kaloshkin, I.A. Tomilin. Thermochimica Acta **280/281**, 303 (1996). https://doi.org/10.1016/0040-6031(96)02926-7

[5] D.V. Louzguine-Luzgin, J. Jiang. Metals **9**, *10*, 1076 (2019). https://doi.org/10.3390/met9101076

[6] B.A. Rusanov, V.E. Sidorov, P. Svec, P. Svec Sr, D. Janickovic, S.A. Petrova. Inorg. Mater. **56**, *1*, 14 (2020).

[7] G.G. Goransky, B.B. Hina, V.I. Zhornik, A.I. Pobol. Vestnik of Vitebsk Technological University **27**, 126 (2014). (in Russian).

[8] C. Parra-Velásquez, D. Perea-Cabarcas, F.J. Bolivar. Revista Facultad de Ingeniería Universidad de Antioquia **95**, 44 (2020).

[9] H. Dhurandhar, A.T. Patel, T.L.S. Rao, K.N. Lad, A. Pratap. J. ASTM Int. **7**, *10*, 1 (2010). https://doi.org/10.1520/JAI102577

[10] S.M. Sarge, G.W.H. Höhne, W.F. Hemminger. Calorimetry. Fundamentals Instrumentation and Applications. Wiley-VCH Verlag GmbH & Co. KGaA: Weinheim, Germany (2014). 280 p.

[11] H.E. Kissinger. Analytical Chem. **29**, *11*, 1702 (1957). https://doi.org/10.1021/ac60131a045

[12] I. Guyzov, S. Toschev. In: Advances in Nucleation and Crystallization in Glasses / Eds L.L. Hench, S.W. Freiman. Am. Ceram. Soc., Inc. (1971). P. 10–23.

[13] V.M. Ievlev, S.V. Kannykin, T.N. Il'inova, M.S. Volodina, E.V. Bobrinskaya, A.S. Baikin, V.V. Vavilova, D.V. Serikov. Inorg. Mater. **52**, *7*, 677 (2016).

[14] R.A. Nazipov, A.V. Mitin, N.A. Zyuzin. Uchenye zapiski Kazanskogo gosudarsvennogo universiteta. Ser. Fiz.-Mat. Nauki **147**, *kn. 2*, 80 (2005). (in Russian).

[15] K. Hono, D.H. Ping. Mater. Characterization **44**, *1–2*, 203 (2000).

[16] E. Jakubczyk, L. Krajczyk, P. Siemion, M. Jakubczyk. Optica Applicata **XXXVII**, *4*, 359 (2007).

[17] G. Abrosimova, A. Aronin, D. Matveev, E. Pershina. Mater. Lett. **97**, 15 (2013).

[18] E.N. Zanaeva, A.I. Bazlov, E.V. Ubyivovk, D.A. Milkova. Phys. Metals. Metallogr. **124**, *6*, 537 (2023).

[19] Yu.N. Goichenberg, V.E. Roshchin, S.I. Il'in. Vestnik YuUrGU. Ser. Metallurgiya **16**, *3*, 134 (2016). (in Russian).

[20] K. Yang, B. Li, X.-H. Fan, X. Wang. J. Therm. Anal. Calorimetry **148**, *3*, 689 (2023). https://doi.org/10.1007/s10973-022-11778-7

[21] S. Sharma, C. Suryanarayana. J. Apl. Phys. **102**, *8*, 083544 (2007). https://doi.org/10.1063/1.2800840

[22] W.F. Gale, T.C. Totemeier. „Smithhells Metal Reference", 8th Edition, Butterworth-Heinemann, Waltham, (2004), 2080 p.

[23] A.M. Gleser, I.E. Permyakova. Materialovedenie, **6**, 30 (2006). (in Russian).

[24] P.J. Van Ekeren. In: Handbook of Thermal Analysis and Calorimetry; v. l. / Ed. M.E. Brown. Elsevier Science B.V. (1998). P. 75–84.

[25] Introduction to Thermal Analysis / Ed. M.E. Brown. Kliwer Academic Publishers, New York, Boston, Dordricht, London, Moscow (2001). 264 p.

[26] V.A. Aleshkevich. Molekulyarnaya fizika. Fizmatlit, M. (2016). p. 307. (in Russian).

[27] J. Piatkowski, V. Przeliorz, V. Szymszal. Archives. Foundry Eng. **17**, *2*, 207 (2017).

[28] J. Šesták. Thermophysical Properties of Solids. Measurments. Their Theoretical Thermal Analysis. Academia Prague (1984). 456 p.

[29] A.K. Galwey, M.E. Brown. Handbook of Thermal Analysis and Calorimetry, v. 1 / Ed. M.E. Brown. Elsevier Science B.V. (1998). 147 p.

[30] I.M. Lifshitz, V.V. Slezov. JETP **8**, *2*, 331 (1959).

[31] P. Haasen. Physikalische Metallkude. Springer Verlag, Berlin (1984). 342 p.

[32] S.V. Terekhov. Phys. Metals. Metallogr. **121**, *7*, 664 (2020).

[33] S. Lesz, R. Nowosielski, B. Kostrubiec, Z. Stoklosa. J. Achievements. Mater. Manufacfurinq Eng. **16**, *1–2*, 35 (2006).

[34] V.S. Kraposhin, V.S. Khmelevskaya, M.Y. Yazvitsky, I.A. Antoshina. J. Non-Cryst. Solids **353**, *32–40*, 3057 (2007).

[35] L.V. Spivak, N.E. Shchepina. Phys. Solid State **61**, *8*, 1347 (2019).

Translated by A.Akhtyamov